Received: 24 January 2024 | Accepted: 25 April 2024

DOI: 10.1111/1365-2745.14342

Journal of Ecology | BRITISH ECOLOGICAL SOCIETY

RESEARCH ARTICLE

Density-dependent influence of ribbed mussels on salt marsh nitrogen pools and processes

Sydney L. Williams[1] | Hallie S. Fischman[1] | Christine Angelini[1] | Ashley R. Smyth[2]

[1]Environmental Engineering Sciences, Engineering School for Sustainable Infrastructure and Environment, University of Florida, Gainesville, Florida, USA

[2]Soil, Water and Ecosystem Sciences, Tropical Research and Education Center, University of Florida, Homestead, Florida, USA

Correspondence
Sydney L. Williams
Email: sydney.williams@ufl.edu

Funding information
Directorate for Biological Sciences, Grant/Award Number: 1652628; Office for Coastal Management, Grant/Award Number: NA20NOS4200119; NSF BIO OCE GCE LTER

Handling Editor: A. Randall Hughes

Abstract

1. Bivalves are becoming an increasingly popular tool to counteract eutrophication, particularly in vegetated coastal ecosystems where synergistic interactions between bivalves and plants can govern important N sequestration pathways. In turn, new calls to evaluate how bivalve densities modify N pools and processes across multiple scales have surfaced.
2. Ribbed mussels, *Geukensia demissa*, and their relationship with smooth cordgrass present a classic demonstration of positive bivalve-plant interactions and offer a useful model for assessing density dependence. We measure porewater ammonium concentrations, N stable isotope signatures in cordgrass tissue, and sediment N fluxes in mussel aggregations and in cordgrass-only plots across a southeastern U.S. salt marsh.
3. In addition to measuring the effect of mussel presence, we evaluate mussel density dependence through a multiscale approach. At the patch scale, we quantify mussel density effects within their aggregations (individuals m^{-2}) while at a larger landscape scale, we quantify mussel density effects on the cordgrass-only areas they neighbour (individuals ~30 m^{-2}).
4. Porewater ammonium concentrations were halved in mussel biodeposits relative to sediments in cordgrass-only areas and negatively related to mussel density within aggregations. Leaf clip $\delta^{15}N$ signatures were nearly 2‰ higher in cordgrass growing among mussel aggregations and increased with increasing patch mussel density. Microcosm incubations showed that mussels enhanced N_2 flux (i.e., nitrogen removal) and DIN flux (i.e., N regeneration) into the water column, where only nitrogen removal increased with increasing patch-scale mussel density. Across the marsh landscape, mussel coverage drove ammonium accumulation and N_2 flux in sediments.
5. *Synthesis*. Our results suggest that, at the patch scale, mussels stimulate the microbial metabolism of N, the assimilation of this bioavailable N by cordgrass, and nitrogen removal in a positive, density-dependent manner. Tidal currents redistribute mussel biodeposits from mussel aggregations to surrounding areas, influencing biogeochemical transformations at scales beyond their physical footprint. We emphasize that the N regeneration potential of bivalve populations is a

significant metric contributing to their mitigation potential and that bivalve density effects may be non-linear, vary across patch to ecosystem scales, and have differing implications for the plants with which they interact.

KEYWORDS
biodeposition, bivalve, denitrification, density-dependence, eutrophication, nitrogen, vegetated coastal ecosystem

1 | INTRODUCTION

The prolonged, human-derived surplus of nitrogen (N) entering watersheds has triggered eutrophication and its consequences (e.g., algal blooms, deoxygenation, submerged aquatic vegetation loss) in many of the world's lakes, estuaries, and nearshore marine ecosystems (Gilbert & Burford, 2017; Wurtsbaugh et al., 2019). It is now clear that N regulation at both the pollutant's sources and receiving ends are paramount to improving aquatic and marine ecosystem health and service provisioning (Desmit et al., 2018). In coastal systems, one prominent strategy may involve the conservation, restoration, and/or aquaculture of suspension feeding bivalves (e.g., mussels, clams, and oysters) to promote N uptake and removal (Ayvazian et al., 2021; Galimany et al., 2017). Complementing land-based mitigation approaches to eutrophication, this nature-based solution is gaining attention and investment from various stakeholder groups. For instance, blue mussel (*Mytilus edulis*) farming operations are considered cost-effective measures for nutrient extraction and water clarity enhancement in the Baltic Sea (Gren et al., 2009; Kotta et al., 2020; Lindahl et al., 2005; Schröder et al., 2014). Bivalve-mediated N regulation may be particularly important in vegetated coastal ecosystems, such as salt marshes, mangrove forests, and seagrass meadows, where synergistic interactions between bivalve populations and macrophytes may govern N sequestration pathways (Gagnon et al., 2020; Gobler et al., 2022). As applications of bivalve bioremediation grow, new calls to evaluate how bivalve densities modify N pools and processes across multiple scales have surfaced (Kellogg et al., 2014; Testa et al., 2015).

Bivalves modify estuarine N cycling through several pathways associated with suspension feeding and biodeposition, and these processes may correlate with bivalve density. Bivalves feed on N-rich seston and transport this material to the benthic environment in the form of biodeposits. Upon mineralization, biodeposits augment inorganic N (i.e., ammonium) availability for macrophyte uptake and, in turn, N storage in macrophyte tissues (Bertness, 1984; Carroll et al., 2008; Reusch et al., 1994). Additionally, biodeposition can enhance nitrification (i.e., microbial oxidization of ammonium to nitrate) as well as denitrification (i.e., microbial reduction of nitrate to inert nitrogen gas), the latter resulting in the removal of N from a system (Bilkovic et al., 2017; Jones et al., 2011; Smyth et al., 2013, 2015) (Figure 1a). Bivalves can also reduce water column turbidity—a critical driver of primary production, and in turn N uptake, by subtidal macrophytes like seagrass (Bulmer et al., 2018; Gobler et al., 2022; Peterson & Heck, 2001). These contributions to N pathways may increase with increasing bivalve density, indicating positive density dependence (Kellogg et al., 2014; Marinelli & Williams, 2003; Sandwell et al., 2009). Positive density dependence underpins other bivalve processes, including interspecific facilitation (Bertness, 1984; Wagner et al., 2012); water filtration (Zhou, Yang, et al., 2006); sediment stabilization and accretion (Allen & Vaughn, 2011; Carss et al., 2020; Ciutat et al., 2007; Crotty et al., 2023); and carbon sequestration (Fodrie et al., 2017). As bivalves facilitate foundational vegetation, they may also bolster a habitat's capacity to support higher population densities of their own conspecifics and, in turn, drive positive feedbacks on their ecosystem service provisioning (Moore & Hughes, 2023). Indeed, positive density dependence often generates intraspecific or self-facilitation feedbacks (Bertness & Callaway, 1994; Bruno et al., 2003; Temmink et al., 2023) and N sequestration services provided by these faunal engineers may similarly respond in a positive direction.

Importantly, however, bivalve-mediated ecosystem functions and services can be modified by their aggregation and/or population density (Allen & Vaughn, 2011; Jones et al., 2011; Wagner et al., 2012). Nitrogen removal (i.e., denitrification) rates may respond parabolically to increasing bivalve density by plummeting at extremely high or low bivalve densities (Lunstrum et al., 2018; Newell, 2004) or may instead plateau among populations with relatively low coverage, as seen with biomass density in restored oyster reefs (Kellogg et al., 2014). Together, these studies suggest that denitrification increases with increasing bivalve density until a density threshold is met, at which point net N flux may shift away from N removal towards regeneration due to excretion and organic matter loading to sediments. Regeneration involves the addition of dissolved inorganic nitrogen (DIN) to the overlying water column that is bioavailable to pelagic primary producers (Figure 1a). Thus, by potentially refuelling instead of controlling algal growth, relatively high bivalve densities may alter the direction and/or strength of bivalve-mediated functions (Booth & Heck, 2009; Murphy et al., 2015; Newell, 2004). Extrapolating rates from experiments to larger scales therefore presumes that these functions scale linearly with density and ultimately limits our capacity to assess bivalve influence at the ecosystem level (Smyth et al., 2018). Despite these complexities and constraints—and despite the growing attention given to bivalves as bioremediation tools for eutrophication—few studies have assessed density-dependent effects of suspension feeders on N cycling, especially

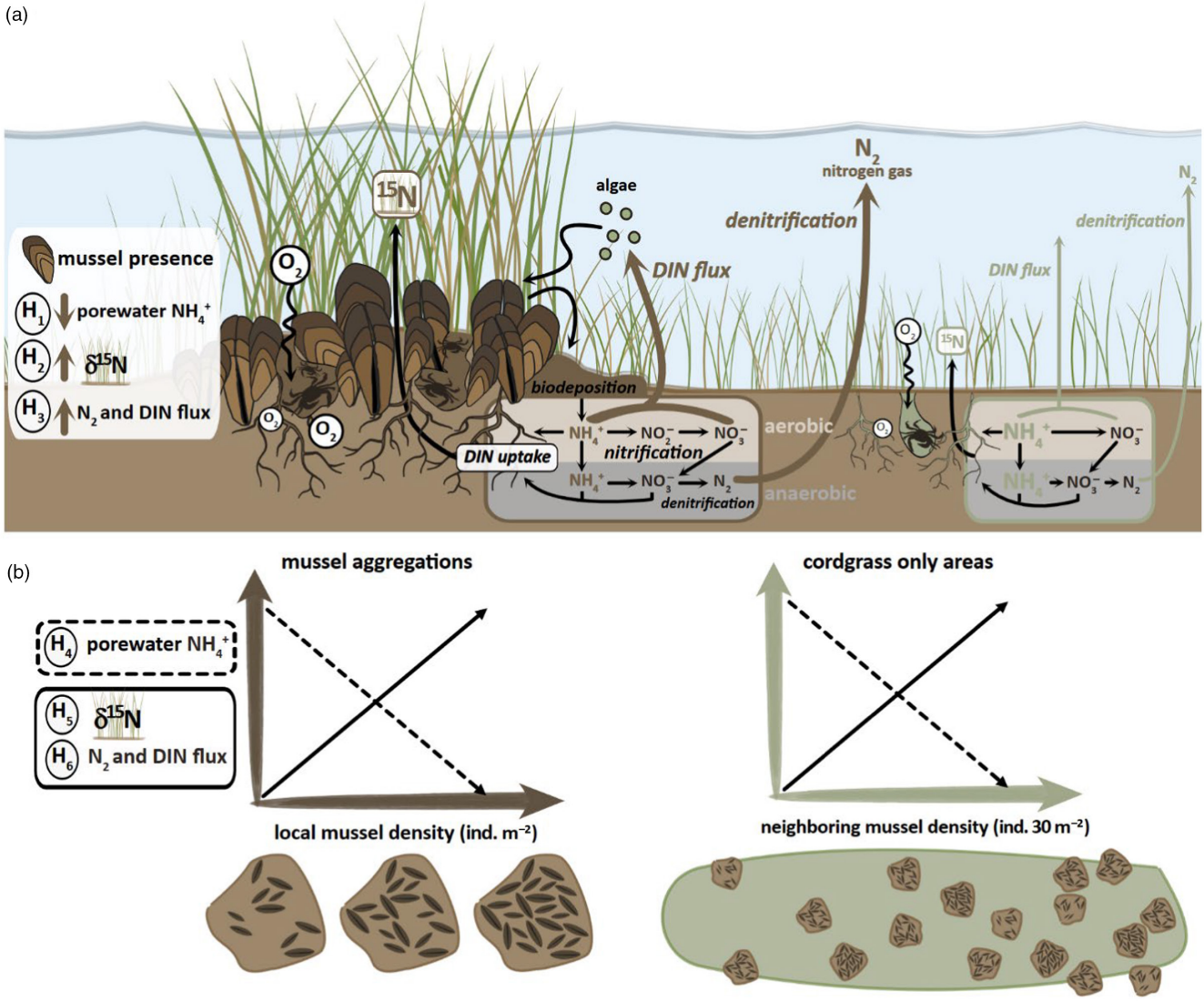

FIGURE 1 Conceptual diagram illustrating the effects of mussel presence (a) and mussel density (b) on N pools and processes. Mussels enhance primary and secondary production within their aggregations, which increases oxygen intrusion into sediments. Coupled with ammonium supplementation via biodeposit decomposition, these processes may increase: nitrification and denitrification in aerobic (beige) and anaerobic (light grey) sediment layers, respectively; ^{15}N assimilation in cordgrass tissues; and dissolved inorganic nitrogen (DIN) and N_2 flux into overlying, tidal waters. Geochemical variables measured in this study are shown for mussel aggregations (brown) and cordgrass-only plots (light green), with font size and line thickness scaled in each area type based on hypotheses H_1, H_2, and H_3 (a). Hypothesized effects of patch and neighbouring mussel density on porewater ammonium (dashed lines; H_4), cordgrass $\delta^{15}N$, and N fluxes (solid lines; H_5 and H_6) in mussel aggregations and cordgrass-only areas, respectively, are also shown (b). Some symbols are courtesy of the Integration and Application Network (ian.umces.edu/symbols/), University of Maryland Center for Environmental Studies.

of those associated with macrophytes (Hoellein & Zarnoch, 2014; Smyth et al., 2015). Though valuable contributions, a majority of prior studies consider intensive aquaculture scenarios defined by extreme bivalve densities that are far higher than those found in natural systems (Carlsson et al., 2012; Humphries et al., 2016; Lunstrum et al., 2018; Murphy, Anderson, et al., 2016; Murphy, Emery, et al., 2016; Nizzoli et al., 2006; Smyth et al., 2018). This nearly exclusive focus on aquaculture has left a gap of understanding around N processes at bivalve densities that represent natural distributions or those targeted in restoration efforts. Thus, it is imperative that density-dependent effects are quantified across the spectrum of bivalve-plant interactions and at multiple scales to best inform nutrient management approaches and coastal restoration efforts more broadly.

Ribbed mussels, *Geukensia demissa* (hereafter, 'mussels') and their relationship with smooth cordgrass (*Spartina alterniflora*; hereafter 'cordgrass') present a classic demonstration of naturally occurring, positive bivalve-plant interactions (Angelini et al., 2016; Bertness, 1984; Bertness & Leonard, 1997) and offer a useful model for assessing density dependence in bivalve-mediated N availability and removal. In the southeastern US where this study is focused, mussels typically form clumped aggregations embedded in the mud

around cordgrass stems and cover 0.2%–1.1% of intertidal salt marsh platforms (Angelini et al., 2015; Stiven & Gardner, 1992). Several investigators to date have measured elevated rates of nitrification and denitrification associated with mussel aggregations (Bilkovic et al., 2017; Fischman et al., 2023; Zhu et al., 2019) (Figure 1a). These mussel-mediated processes may increase with mussel density within aggregations given that these organisms fuel a positive, density-dependent feedback system of N supplementation, primary and secondary production, and oxygenation within their aggregations (Angelini et al., 2015; Bertness, 1984; Derksen-Hooijberg et al., 2018; Williams et al., 2023) (Figure 1b). In addition to locally priming sediments for enhanced nitrogen bioavailability and removal, mussel biodeposits are redistributed by tidal currents to areas surrounding their aggregations (Crotty et al., 2023) and may in turn influence biogeochemical transformations in salt marshes at scales beyond their physical footprint (Figure 1b). Therefore, mussels can potentially act as a N removal tool in salt marsh estuaries, but understanding how these mussel-mediated functions scale along density gradients both within aggregations and across the broader marsh landscape is critical for informing future management and restoration efforts.

Here, we measure mussel influence on N cycling in salt marshes by quantifying porewater ammonium concentrations, N stable isotope signatures in cordgrass tissue, and sediment N fluxes in mussel aggregations growing among cordgrass and in 0.25 m^2 cordgrass-only plots. Based on previous evidence for mussel-enhanced nitrification and denitrification, we first hypothesize that mussel presence decreases porewater ammonium concentrations in biodeposit layers and in sediments underneath mussel aggregations relative to surface sediments in cordgrass-only areas (H_1). Our next hypothesis considers the assimilation of this microbially transformed N by cordgrass, asserting that $\delta^{15}N$ values in aboveground cordgrass tissues will be higher in plants growing among mussels relative to those growing without mussels (H_2). Tested through microcosm incubations, we then hypothesize that N_2 flux (i.e., denitrification) and DIN flux are higher in mussel biodeposits than in cordgrass-only sediments (H_3). In addition to considering the effect of mussel presence (Figure 1a), we evaluate mussel density dependence of these processes through a multi-scale approach (Figure 1b). At the patch scale, we quantify the effect of mussel density on N cycling within their aggregations (hereafter 'patch density', individuals m^{-2}). At a larger landscape scale, we quantify the effect of mussel density on N cycling in the cordgrass-only areas they neighbour (hereafter 'neighbouring density', individuals ~30 m^{-2}). Our hypotheses related to density-dependent effects assert that porewater ammonium concentrations decrease (H_4), while leaf $\delta^{15}N$ values (H_5) and N_2 and DIN fluxes (H_6) increase, with increasing patch and neighbouring mussel density in mussel aggregations and cordgrass-only areas, respectively. Collectively, this work expands our understanding of bivalve-plant interactions and how they modify N pools and processes, including sequestration, in salt marsh systems particularly by contributing new insight into the density-dependent mechanisms underpinning these relationships.

2 | MATERIALS AND METHODS

2.1 | Mussel density and salt marsh community surveys

This study was conducted on the higher elevation, interior platforms of a salt marsh adjacent to Old Teakettle Creek near Sapelo Island, GA (31.451999, −81.317059) (Figure S1). Marsh platforms in this region are characterized by intertidal creeks that stem from larger main channels. The site floods and drains semidiurnally via Doboy Sound and is tidally inundated for ~6 h per day. Doboy Sound receives fresh- and saltwater input from the Altamaha River and the Atlantic Ocean, respectively. Mussel distribution and vegetation structure along Old Teakettle Creek were typical of salt marshes in southeastern US estuaries, with the highest mussel densities at mid-elevation platforms (i.e., short form cordgrass) surrounding the heads of intertidal creeks (Annis et al., 2022; Crotty & Angelini, 2020; Kuenzler, 1961; Lin, 1989). In summer 2017, a mussel manipulation was performed at the site as described in Williams et al. (2023). All mussels from one interior marsh platform (~1000 m^2) were carefully excavated and transplanted to another, directly adjacent platform of similar size, while a third, adjacent platform was left undisturbed. This manipulation resulted in a gradient of mussel cover across the site (i.e., excavated, transplanted, and undistributed).

In 2020, 3 years after the mussel manipulation, we selected the site to leverage its gradient of mussel cover and, in turn, measure mussel density effects at a landscape scale. A Letter of Authorization and Revocable Licence (RLS20190024) were attained from the GA Department of Natural Resources for this study in June 2019. We first randomly selected mussel aggregations growing at the base of cordgrass stems and 0.25 m^2 cordgrass-only plots across the mussel cover gradient ($n = 40$ per mussel aggregations and cordgrass-only plots). Mussel aggregations ranged between 0.1 to 4.3 m^2 across the study site, averaging 1.07 m^2 (±1.05; SD) in size. Cordgrass-only plots were located at least 1 m away from any mussel aggregation. In each aggregation and plot, we counted crab burrows and live cordgrass stems that fell within a 0.25 m^2 quadrat and measured the vertical extent of mussel biodeposit layers by pushing a meter stick into the centre of each aggregation until it hit refusal. We surveyed mussel density in each aggregation by counting all surficial mussels within an aggregation and computed patch scale densities as individuals m^{-2}. We also surveyed neighbouring mussel density by counting all mussels residing within a 3 m radius from the centre of each cordgrass-only plot, which ranged from 0 to approximately 700 individuals (ind. 9πm^{-2}).

2.2 | Porewater ammonium sampling and analysis

To test the hypotheses that mussel presence and patch and neighbouring mussel density decreases porewater ammonium concentrations (H_1 and H_4), we measured porewater ammonium concentrations (μM) in the biodeposit layer of mussel aggregations as well as in sediment underneath mussel aggregations and in cordgrass-only plots. Porewater was collected during the summer season when mussel suspension feeding and biodeposition are most active. We collected porewater by inserting a Rhizon sampler (0.60 μm; Rhizosphere Research Products) in the biodeposit and sediment layers (5 and 10 cm in depth, respectively). Biodeposit porewater was randomly subsampled from the selected mussel aggregations with biodeposit depths >1 cm ($n = 5$ aggregations) while sediment porewater was collected in all selected mussel aggregations and cordgrass-only plots ($n = 40$ per area type). We stored the porewater samples on ice during transport to the lab and then immediately filtered them through a 0.45 μm syringe filter into 20 mL scintillation vials. The samples were kept frozen until we measured their ammonium concentrations on a SEAL AutoAnalyzer 3 HR at the University of Florida's Fort Lauderdale Research and Education Center (FLREC). Here and below, the SEAL detection limit for NH_4^+ was 0.040 μM.

2.3 | Isotopic analysis of foundational salt marsh vegetation

To test the hypotheses that mussel presence and patch and neighbouring mussel density increase $\delta^{15}N$ signature of residual DIN pool available for uptake and absorption (H_2 and H_5), we measured bulk N isotopic signatures in cordgrass aboveground biomass. We collected leaves from plants in a subsample of mussel aggregations and cordgrass-only plots ($n = 20$ per area type) by clipping and compositing the second new leaf from 3 stems, rinsing them with deionized water, drying them at 60°C until they reached constant weight, grinding them to a fine powder, and then measuring $\delta^{15}N$ signatures by stable isotope analysis at the University of Florida's Stable Isotope Mass Spectrometry Lab (Costech-DeltaPlusXL IRMS). Stable isotope ratios are hereby expressed in the delta (δ) notation relative to atmospheric nitrogen.

2.4 | Microcosm incubations

To test the hypotheses that mussel presence and patch and neighbouring density increase N_2 and DIN fluxes (H_3 and H_6), we conducted microcosm incubations on biodeposits and sediments collected from a subsample of mussel aggregations and cordgrass-only plots, respectively ($n = 18$ per area type). At low tide, we collected cores from each plot (2.5 cm diameter) and then recorded the number of cores collected per plot and the volume of material collected from each core. Core depth differed across plots due to biogenic structural heterogeneity (i.e., interstitial spacing within live mussels and cordgrass stems and roots) but reached a maximum of 10 cm. We composited the cores into a single whirl-pak® bag for each plot and kept the bags on ice until further processing. Cores collected from mussel aggregations contained biodeposits only, and no live mussels. We also collected 12 L of site water (salinity = 25 ppt) in amber carboys from Old Teakettle Creek which is located adjacent to our marsh site. We stored the whirl-pak® bags in a refrigerator at 4°C overnight and performed the incubations within 24 h of field collection following methods adapted from Reisinger et al. (2016). We homogenized the cores composited in each bag and then added each sediment sample to duplicate 50 mL polypropylene centrifuge tubes for sacrificial sampling at 0, 6, and 10 h at a consistent volume (~10 mL) and weight ($n = 6$ tubes per sediment sample; 108 total tubes). Then we slowly filled each tube with site water using a syringe and capped them underwater in site water buckets to prevent any headspace. Additionally, duplicate tubes were filled with site water only (hereafter 'water blanks') for each incubation time point ($n = 6$ total water blanks) and capped underwater. Incubations were run at 24°C.

We then sacrificially sampled tubes at 0, 6, and 10 h after capping. At each time point, we collected samples for dissolved gas and DIN analyses. We first collected ~40 mL of water with a syringe and slowly transferred it to a 12 mL Exetainer© sample vial (Labco Ltd., Lampeter, UK), allowing most of the sample to overflow out of the vial and into a beaker to attain a positive meniscus and prevent atmospheric contamination. We then added 100 μm of 7 M $ZnCl_2$ to each vial for preservation and stored them at 4°C submerged and upside down prior to dissolved gas analysis. We then filtered the overflowed aliquot through a 0.45-micron syringe filter into a scintillation vial and froze the vials prior to DIN (NH_4^+ and $NO_3^- + NO_2^-$) analysis.

We measured dissolved N_2 and Ar using a membrane inlet mass spectrometer at the University of Florida's Tropical Research and Education Center and calculated concentrations of N_2 using its ratio with Ar (Kana et al., 1994). We determined the change in concentrations of N over time (rate; μmols $N\,h^{-1}$) for the water blank and each plot from simple linear regressions with duplicates treated as individual values (i.e., not averaged) and then corrected for water column changes by subtracting the water blank rate from each plot rate. We then calculated areal $N-N_2$ flux (μmols $m^{-2}\,h^{-1}$) by dividing the rate by the surface area represented by the incubations. Surface area was calculated as $A_{cores} \times V_{incubation}/V_{cores}$ where A_{cores} is total surface area of cores collected in each plot, $V_{incubation}$ is the volume of water in each incubation, and V_{cores} is the total volume of sediment collected in cores at each plot (Reisinger et al., 2016). A net positive N_2 flux indicates that denitrification dominated the total N_2 flux, while a net negative N_2 flux indicates nitrogen fixation dominated. We also measured concentrations of NH_4^+ and NO_x ($NO_3^- + NO_2^-$) on a SEAL AutoAnalyzer 3 HR (FLREC) with a NO_x detection limit of 0.007 μM. We then calculated areal $N-NH_4^+$ and $N-NO_x$ fluxes using the same mathematical approach described above and summed these values to quantify DIN flux for each plot. As sediment gradients were broken up during core homogenization, $N-N_2$ and DIN fluxes represent potential areal rates specifically used for the relative, statistical comparisons described

below. Additionally, while polypropylene tubes have been used for gas fluxes before, there may be diffusion across the plastic, which we assume to be equal across all tubes. Because of these limitations, this microcosm incubation method is an effective tool for drawing relative comparisons between treatments or areas (e.g., mussel aggregations and cordgrass-only plots) as opposed to extrapolating flux measurements to an ecosystem level.

Finally, we determined whether incubation samples drove net N regeneration or removal in the water column based on denitrification efficiency, or the percent of total benthic DIN efflux made up of N_2. Denitrification efficiency was calculated using the following equation (Eyre & Ferguson, 2002): $N-N_2$ flux/(DIN flux + $N-N_2$ flux) × 100. An efficiency greater than 50% indicates that more mineralized nitrogen is being removed through denitrification than regenerated while an efficiency of less than 50% indicates that nitrogen regenerated back to the water column is greater than nitrogen removal (see Figure S3).

2.5 | Hypothesis testing with Bayesian model frameworks

Hypothesis testing was conducted by quantifying the effect size and uncertainty of predictor variables on response variables using Bayesian generalized modelling frameworks. Specifically we measured the effect of: (1) sampling location (i.e., mussel biodeposit layer, mussel sediments, and cordgrass-only sediments) on porewater ammonium concentrations (H_1); (2) area type on $\delta^{15}N$ cordgrass signatures (H_3) and $N-N_2$ and DIN flux (H_5); and (3) patch and neighbouring mussel density on porewater ammonium concentrations (H_2), $\delta^{15}N$ cordgrass signatures (H_4), and $N-N_2$ and DIN flux (H_6). A Bayesian framework allows for a multivariate response approach whereby models can be run directly without data transformations, fit response-specific distributions and link functions, and result in clear effect sizes and uncertainty for each estimated effect. Posterior predictive checks were performed for each response variable to determine best-fit distributions and link functions. Regression models quantifying density-dependent effects of patch and neighbouring mussel density on responses variables measured from mussel aggregations and cordgrass-only plots, respectively, were built as separate frameworks. Model frameworks were built, run, and assessed using Stan (Stan Development Team, 2023) and R (v. 4.3.1; R Core Team, 2023) with the R packages brms (v. 2.19.0; Bürkner, 2017, 2018, 2021), CmdStanR (v. 0.6.0; Gabry et al., 2023), bayesplot (v. 1.10.0; Gabry & Mahr, 2022), and posterior (v. 1.4.1; Bürkner et al., 2023). Effect sizes of sampling locations and area type are presented as estimated median posterior of differences from each Markov Chain Monte Carlo (MCMC) draw with 95% credible intervals (CIs). Lastly, density-dependent effects are presented as median estimates of slope coefficients from each MCMC draw with 95% CIs and Bayesian R^2 values. For all model outputs, 95% CIs are presented in brackets or parentheticals. All model formulas, including response distributions and link functions, estimated coefficients, and uncertainty intervals are summarized in Table S1.

3 | RESULTS

3.1 | Mussel effects on porewater ammonium

Estimated median ammonium concentrations (Figure 2a) were approximately 55% to 65% lower in porewater extracted from the mussel biodeposit layer (90.7 μM [64.9, 128.2]) than from sediment underneath mussel aggregations (158.6 μM [133.9, 190.83]) and in cordgrass-only plots (175.9 μM [149.5, 209.0]) (effect size = −0.53 [−0.91, −0.15] and −0.66 [−1.03, −0.29], respectively), which were similar to one another (−0.13 [−0.36, 0.10]). When considering density-dependent effects of mussels on porewater ammonium (Figure 2b,c), we found that concentrations underneath mussel aggregations generally decreased as a log function with increasing patch mussel density (coefficient = −0.003 [−0.005, −0.0001]; Bayesian R^2 = 0.14 [0.002, 0.36]). However, ammonium concentrations in cordgrass-only sediment porewater was positively related as a log function to neighbouring mussel density (0.001 [0.0005, 0.002]; Bayesian R^2 = 0.25 [0.04, 0.47]).

3.2 | Mussel effects on cordgrass bulk nitrogen signatures

Median estimates of $\delta^{15}N$ signatures of cordgrass growing with mussels (5.84‰ [5.50, 6.17]) were substantially elevated relative to those of cordgrass growing in plots void of mussels (3.95‰ [3.61, 4.28]) (Figure 3a), with a positive effect size of mussel presence nearing 2‰ in posterior differences (1.89 [1.42, 2.36]). Further, patch mussel density explained 50% of the variation in cordgrass $\delta^{15}N$ signatures from plants sampled from mussel aggregations, where $\delta^{15}N$ increased linearly with mussel density within aggregations (0.006 [0.003, 0.009]; Bayesian R^2 = 0.50 [0.17, 0.66]) (Figure 3b). However, neighbouring mussel density had no detectable effect on this metric in cordgrass-only plots (Figure 3c).

3.3 | Mussel effects on net N_2 and DIN fluxes

We measured nearly a 60% increase in $N-N_2$ flux with mussel presence as median estimates increased from 12.44 (9.74, 16.22) μmols $N\,m^{-2}\,h^{-1}$ in cordgrass-only plots to 22.90 (17.72, 30.15) μmols $N\,m^{-2}\,h^{-1}$ in mussel aggregations (0.61 [0.30, 0.92]; Figure 4a). Both patch and neighbouring mussel density were positively associated with net N_2 production in mussel aggregation (0.07 [0.04, 0.11]; Bayesian R^2 = 0.41 [0.07, 0.61]) and cordgrass-only sediments (0.03 [0.02, 0.05]; Bayesian R^2 = 0.42 [0.10, 0.62]), respectively, such that $N-N_2$ flux increased linearly with both mussel density measures (Figure 4b,c). Mussel presence generally promoted the net positive flux of DIN into the water column as median estimates of DIN flux were approximately 200% higher in mussel aggregations (39.41 [5.13, 29.01] μmols $N\,m^{-2}\,h^{-1}$) relative to cordgrass-only samples (7.28 [−2.63, 17.34] μmols

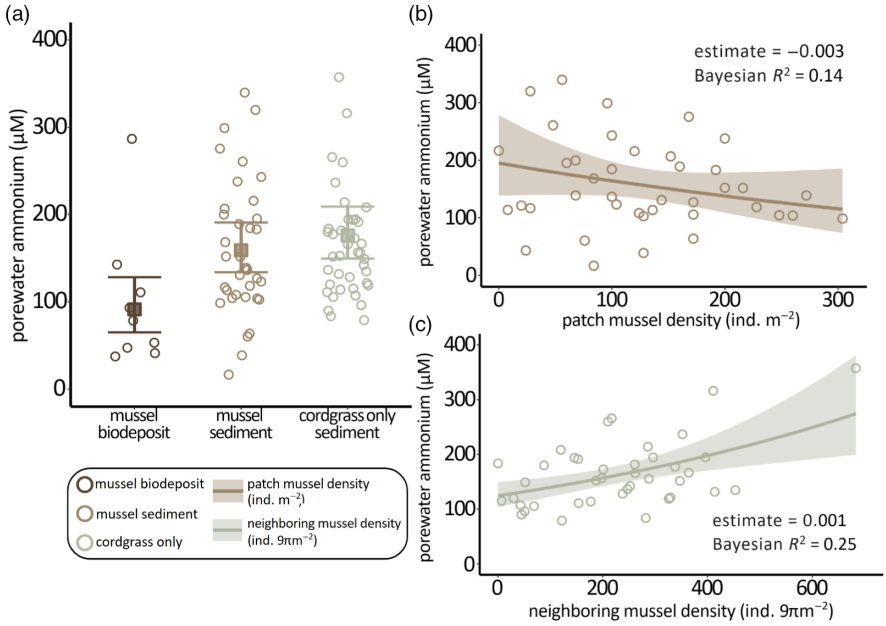

FIGURE 2 Mussel effects on porewater ammonium. Conditional effects plot shows estimated median values (filled squares) of porewater ammonium concentrations (μM) (a) in mussel biodeposits (5 cm in depth; dark brown) and sediments (10 cm in depth) underneath mussel aggregations (light brown) and in cordgrass-only plots (green) with 95% CIs (error bars) and raw data (open points). Generalized regression models of ammonium concentrations in mussel and cordgrass-only sediments against patch (b) and neighbouring (c) mussel density, respectively, are also presented. Median estimates, trend lines, 95% CIs (shaded areas), and Bayesian R^2 values are shown for meaningful predictors. Note that data from panel (a) is shown in (b) and (c) across mussel densities.

FIGURE 3 Mussel effects on cordgrass bulk nitrogen signatures. Conditional effects plot shows estimated median values (filled squares) of $\delta^{15}N$ values (‰) in cordgrass leaves (a) clipped from plants growing among mussel aggregations (light brown) and in cordgrass-only plots (green) with 95% CIs (error bars) and raw data (open points). Generalized regression models of leaf clip $\delta^{15}N$ in mussel and cordgrass-only plots against patch (b) and neighbouring (c) mussel density, respectively, are also shown. Median estimates, solid trend lines, 95% CIs (shaded areas), and Bayesian R^2 values are shown for meaningful predictors. Note that data from panel (a) is shown in (b) and (c) across mussel densities.

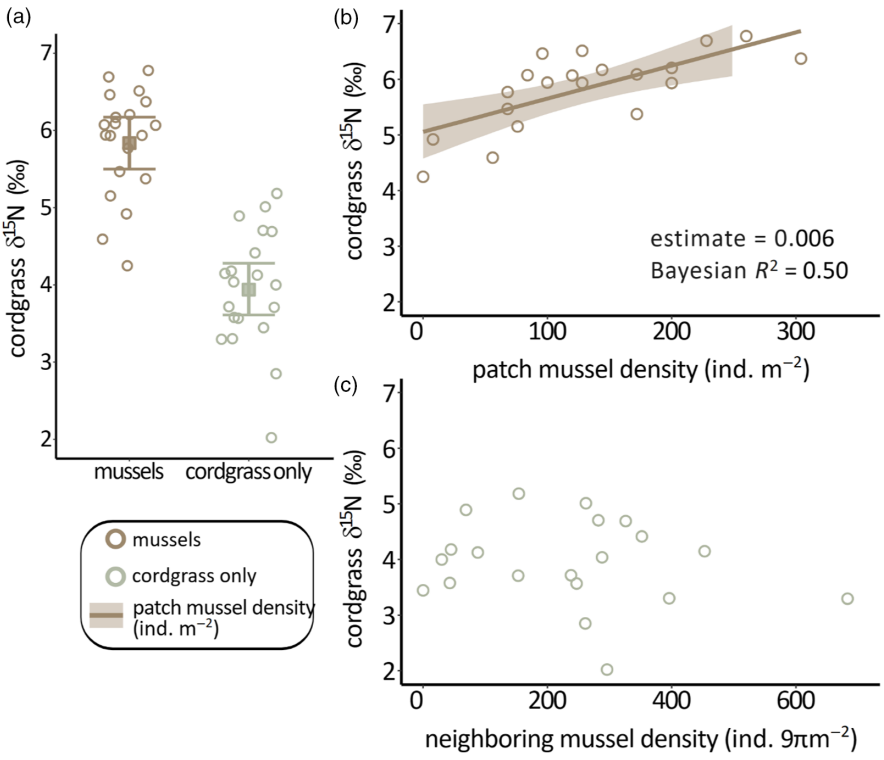

$N\,m^{-2}\,h^{-1}$) (32.07 [20.10, 44.05]) (Figure 5a). $N-NH_4$ flux made up 89.7 ± 2.3% (mean ± SE) of DIN fluxes across all samples. Unlike $N-N_2$ fluxes, DIN flux was unrelated to patch and neighbouring mussel density (Figure 5b,c).

4 | DISCUSSION

Here, we explore mechanistic pathways underpinning N transformations, bioavailability, and flux in sediments and how they differ

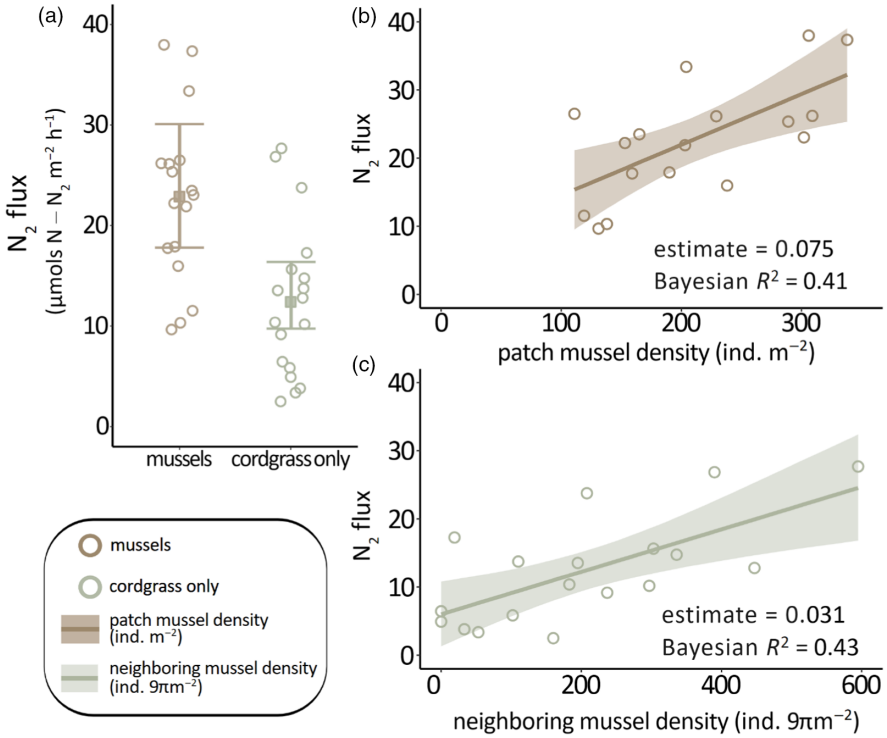

FIGURE 4 Mussel effects on net N_2 fluxes. Conditional effects plots show estimated median values (filled squares) of N_2 (μmols N m^{-2} h^{-1}) during microcosm incubations of mussel (light brown) and cordgrass-only sediments (green) with 95% CIs (error bars) and raw data (open points) (a). Generalized regression models of N_2 flux in mussel and cordgrass-only areas against patch (b) and neighbouring (c) mussel density, respectively, are also presented. Median estimates, solid trend lines, 95% CIs (shaded areas), and Bayesian R^2 values are shown for meaningful predictors. Note that data from panel (a) is shown in (b) and (c) across mussel densities.

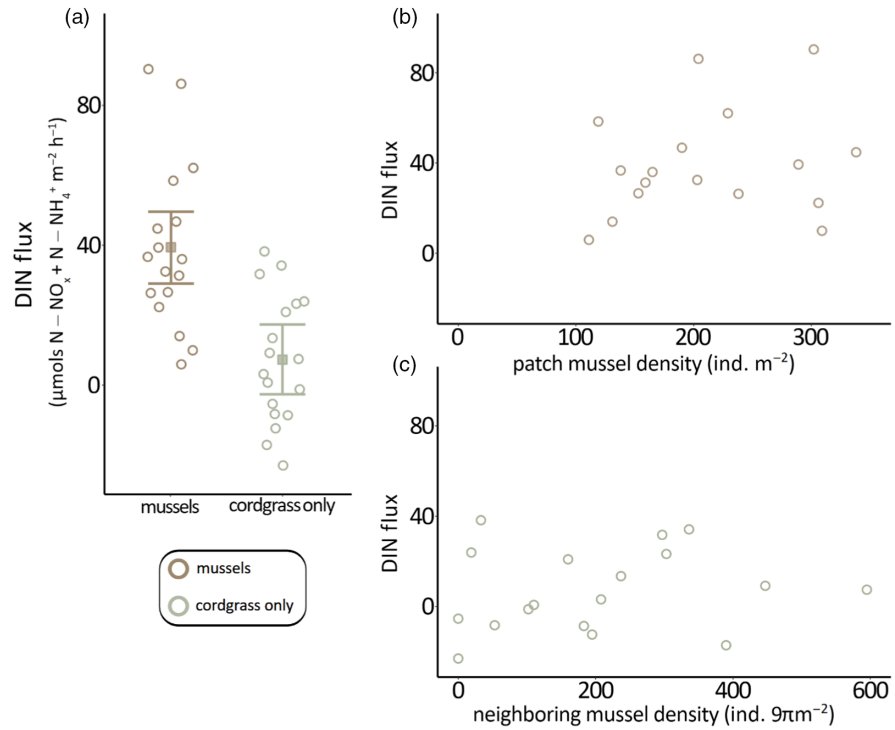

FIGURE 5 Mussel effects on net dissolved inorganic nitrogen (DIN) fluxes. Conditional effects plots show estimated median values (filled squares) of DIN flux (μmols N m^{-2} h^{-1}) during microcosm incubations of mussel (light brown) and cordgrass-only sediments (green) with 95% CIs (error bars) and raw data (open points) (a). Generalized regression models of DIN flux in mussel and cordgrass-only areas against patch (b) and neighbouring (c) mussel density, respectively, are also presented. Note that data from panel (a) is shown in (b) and (c) across mussel densities.

between mussel aggregations and cordgrass-only plots. Mussel presence decreased porewater ammonium concentrations and increased cordgrass $\delta^{15}N$ signatures, denitrification, and N regeneration relative to cordgrass-only plots. With the exception of N regeneration, these biogeochemical indicators also responded strongly in the same direction to increasing patch mussel density. At the landscape scale, porewater ammonium and denitrification increased with increasing neighbouring mussel density. As far as we know, our study is the first of its kind to measure density dependence of nitrogen removal by mussels and to document, for any suspension feeder, the extension of this ecosystem service to the broader vegetated coastal landscape as it relates to their coverage (i.e., neighbouring mussel density). These considerations are critical for effective evaluation of bivalve influence at the ecosystem level.

As this study was conducted across a single salt marsh landscape, we emphasize here and below the importance of addressing site- or region-specific environmental contexts and how these may modify suspension feeder effects in future studies. Collectively, our results contribute to a growing body of work that aims to identify how ecosystem functions mediated by natural or restored bivalve populations scale across varying degrees of bivalve coverage.

4.1 | Mussel biodeposition, positive interactions, and contexts controlling N pools and processes

Porewater ammonium and leaf clip geochemistry (i.e., $\delta^{15}N$ signatures) serve as our first two lines of evidence resolving the role of mussels in N availability and cycling in salt marshes, with both pointing to three principal mechanisms as potential explanations behind their results (Figure 1a). First, mussels and the benthic invertebrates they facilitate, such as juvenile fiddler crabs and purple marsh crabs, augment pore space and sediment oxygenation in the biodeposit layer via their excavation of burrows (Angelini et al., 2015; Derksen-Hooijberg et al., 2018). Enhanced oxygen intrusion by these bioturbators can in turn promote nitrification (Laverock et al., 2011). Corroborating previous evidence of indirect oxygenation by mussels, our study found nearly a 20-fold increase in crab burrow densities (no. burrows 0.25 m^{-2}) in mussel aggregations (73 ± 5; mean ± SE) relative to cordgrass-only plots (4 ± 1) (Figure S2a). Second and along a similar vein, mussels promote belowground cordgrass production in the rhizosphere (Bertness, 1984; Derksen-Hooijberg et al., 2018)—a region responsible for oxygen transport and the stimulation of coupled nitrification–denitrification (Matheson et al., 2002). Indeed, cordgrass root and rhizome biomass were 100% higher in mussel aggregations relative to cordgrass-only areas and positively density dependent at the patch scale (ind. m^{-2}) during a previous study at the same site (Williams et al., 2023). We therefore might also expect enhanced oxygenation and N removal with mussel presence and increasing patch density in part due to higher cordgrass root and rhizome biomass. Lastly, the decomposition of mussel biodeposits supplements the oxygenated marsh surface with ammonium. This process promotes nutrient uptake by cordgrass roots and/or shifts microbial metabolism towards pathways of ammonium oxidation (Bilkovic et al., 2017). Our geochemical findings discussed below may largely be explained by these mechanisms underpinned by mussel biodeposition and their positive, ecological interactions with other salt marsh community members.

Within aggregations, porewater ammonium concentrations were halved (i.e., 55%–65%) in mussel biodeposits relative to sediments from both area types and negatively related to patch mussel density. Given the higher ammonium absorption and oxidation present in sediments directly engineered by mussels, we would expect a depletion of bioavailable N in the highly aerobic and active biodeposit layer relative to typical salt marsh sediments that are poorly oxygenated and support lower crab abundances and belowground cordgrass biomass (H_1). Dissimilatory nitrate reduction to ammonium (DNRA) in these more anaerobic, sulfidic sediments is also likely contributing to their higher porewater ammonium concentrations (Koop-Jakobsen & Giblin, 2010; Smyth et al., 2013). Contrary to our first hypothesis, ammonium concentrations were indistinguishable between sediments below the mussel biodeposit layer (i.e., 10 cm in depth) and those in cordgrass-only plots—a finding that is likely attributed to lower organic matter loading (via biodeposition) and oxygen intrusion into this deeper soil horizon. In turn, muted pathways of mineralization and ammonium oxidation (i.e., nitrification) and/or elevated pathways of ammonium production (i.e., DNRA) may be more prevalent in sediments underneath mussel aggregations. However, we did discern negative density dependence in the distribution of ammonium concentrations in these sediments at the patch scale (H_4), which may point to a trickle-down effect of mussel-enhanced nitrification on bioavailable N pools in deeper sediment layers that increases with increasing mussel density. Indeed, past studies have shown positive relationships between conditions that prime sediments for nitrification (i.e., biodeposition, bioturbator abundance, infiltration, and cordgrass belowground biomass) and mussel density within aggregations (Angelini et al., 2015; Crotty et al., 2023; Williams et al., 2023).

Meanwhile, we detected that mussel density effects change direction at the landscape scale, such that porewater ammonium concentrations in cordgrass-only sediments increased as neighbouring mussel coverage increased. This contrasting relationship between mussel density and ammonium concentrations at patch versus landscape scale may be in part explained by the dispersal of biodeposits to the surrounding salt marsh platform, followed by the accumulation of ammonium upon their decomposition. We propose that this mechanism of ammonium accumulation may be largely driven by the lower incidence of bioturbation, belowground cordgrass biomass, oxygenation, and nitrification in salt marsh areas unsupported by mussel biogenic structure. In short, mussel presence and density stimulate the cycling and uptake of ammonium within mussel aggregations, yet increased landscape-scale mussel densities may contribute to buildup of ammonium in cordgrass-only areas. Additionally, stress and disturbance may be important factors to consider here. At the time of porewater sampling, cordgrass-only plots at our site presented symptoms of a moderate dieback event (i.e., thinning; high densities of standing dead cordgrass) (C. Angelini, *pers. obs.*), with mean (±SE) live stem densities (110 ± 10 stems m^{-2}; Figure S2b) nearing those surveyed in dieback studies of Georgia mid-marsh, short form cordgrass sites (Alber et al., 2008; Ogburn & Alber, 2006). Ammonium levels are often elevated in soils associated with dieback relative to healthy marshes, as this form of nitrogen accumulates when cordgrass roots and rhizomes experience stress, degrade, and fail to take up bioavailable N (Goodman & Williams, 1961; Ogburn & Alber, 2006; Sharp & Angelini, 2016). Thus, mussel biodeposition, decomposition of organic cordgrass tissue, and low ammonium uptake rates by stressed cordgrass stands may act as compounding mechanisms of ammonium accumulation.

For instance, Derksen-Hooijberg et al. (2018) measured substantially higher porewater ammonium concentrations in dieback sediments with mussel transplants (307 ± 29 μM) relative to areas left void of mussels (186 ± 30 μM). We therefore highlight the importance of considering density-dependent biodeposit dispersal and how the direction and magnitude of a suspension feeder's role in vegetated coastal ecosystems can shift in various contexts, including during periods of stress and disturbance.

Our second line of evidence for mussel-mediated N availability and flux showed that $\delta^{15}N$ signatures of cordgrass tissues were substantially higher (by nearly 2‰) in plants growing among mussel aggregations (H_2), increased with increasing patch mussel density and exhibited no relationship with neighbouring mussel density (H_5). In the context of bulk stable isotopes, dissimilatory reactions, such as ammonification, DNRA, nitrification, and denitrification, preferentially use the lighter ^{14}N over the heavier ^{15}N (Fry, 2006). In estuarine sediments, this isotope fractionation results in the accumulation of ^{15}N in residual, labile N pools available for absorption by cordgrass, which can result in higher $\delta^{15}N$ signatures in its tissues (Brandes & Devol, 1997; Thornton & McManus, 1994; Zhou, Wu, et al., 2006). Although our isotopic approach does not resolve relative rates of DIN transformations (e.g., nitrification, denitrification, DNRA), it reinforces our conclusion that mussels locally stimulate the microbial metabolism of N and indicates that a portion of this bioavailable DIN is assimilated by cordgrass. Further, our results reveal positive density dependence underpinning this mussel-stimulated N availability to and use by cordgrass at the patch scale. Previous studies have attributed this mechanism of cordgrass facilitation by mussels to their positive, density-dependent biodeposition (Angelini et al., 2015; Bertness, 1984; Rossi et al., 2022; Williams et al., 2023). Meanwhile, the uniform distribution of leaf clip $\delta^{15}N$ signatures in cordgrass-only plots across neighbouring mussel density further corroborates our interpretation of porewater ammonium results at this larger sale. Despite receiving density-dependent inputs of ammonium from neighbouring mussels, cordgrass in these plots is unable to absorb and assimilate this supplemental, labile N at detectable isotopic levels without the facilitative support provided by mussels.

4.2 | Direct measures of mussel-enhanced nitrogen removal and trade-offs of nitrogen regeneration

While allowing for direct measures of N fluxes, our microcosm incubations offer an opportunity to draw relative comparisons between mussel aggregations and cordgrass-only areas and to quantify how this function scales along multiple density gradients. First, these data revealed substantially enhanced denitrification in mussel sediments relative to those collected in cordgrass-only plots (H_3), aligning with past studies that quantified the highest denitrification rates in areas containing live mussels with marsh grass and sediment (Bilkovic et al., 2017; Zhu et al., 2019). Denitrification was also prominently and positively density-dependent at both the patch and landscape scale (H_6)—a finding that generally corroborates the scant studies that have measured this relationship with oyster densities (Hoellein & Zarnoch, 2014; Kellogg et al., 2014; Smyth et al., 2015). Interestingly, denitrification scaled linearly across our study's mussel density gradients, which can be defined as moderate to high given that average patch densities (141 ± 12 ind. m^{-2}) fell well above a threshold (16 ind. m^{-2}) previously determined for high mussel coverage in Georgia salt marshes (Annis et al., 2022). Positive density dependence of nitrogen removal is likely driven by similarly dependent mechanisms of enhanced nitrification (see Section 4 above; Figure 1a) that increase nitrate availability for denitrification via anaerobic microbial metabolism (Bilkovic et al., 2017; Laverock et al., 2011; Matheson et al., 2002). Indeed, nitrification is often coupled with denitrification and many investigations to date have found a positive correlation in the magnitude of these two processes (e.g., Aziz & Nedwell, 1979; Kaplan et al., 1979; Kemp et al., 1990). Similarly, positive, density-dependent findings at the broader scale (i.e., neighbouring density) align with those determined through porewater ammonium analyses, collectively indicating that physical processes of biodeposit redistribution from mussel aggregations can lead to DIN supplementation, and ultimately its removal in the form of inert gas, in the surrounding cordgrass matrix.

Alternatively, supplemental organic matter in salt marsh sediments, like biodeposits, can experience higher rates of nitrogen regeneration, an opposing fate to nitrogen removal (Figure 1a). Indeed, despite driving elevated denitrification, mussel sediment incubations also showed substantially more positive benthic DIN efflux (H_3)—and more commonly drove net N regeneration (~80% of samples; Figure S3a), where DIN flux exceeded that of N_2—relative to cordgrass-only sediment incubations (~40% of samples; Figure S3b). Mussel incubation treatments have previously functioned as a source for inorganic N to the water column, with denitrification efficiencies falling to a minimum (14.14% ± 1.08) in cores containing only live mussels (Bilkovic et al., 2017). However, while commercial-scale bivalve aquaculture (i.e., extreme bivalve density) has repeatedly been shown to fuel local nutrient enrichment and primary production in the water column (Bartoli et al., 2003; Murphy et al., 2015), DIN fluxes measured here were unrelated to both scales of mussel density (H_6). This uniform distribution of DIN flux even extended to salt marsh areas that supported effectively double the mussel coverage from transplantation relative to the density that occurred naturally across the control platform. Collectively, our flux results suggest that salt marsh N functioning mediated by natural mussel populations, even those at relatively high degrees of coverage, may not exceed density thresholds at which net N removal switches to net N regeneration.

4.3 | Considerations for management of eutrophic estuaries

As estuaries worldwide face threats of excessive nitrogen loading, bivalves are becoming increasingly popular tools for bioremediation. Potentially compounding or modifying the effects of bivalve density,

environmental contexts, such as drought stress or nutrient enrichment status, are also important determinants of a population's N service provisioning. For example, although a positive relationship was found between natural oyster density and N_2 production across habitat types (i.e., mudflat, salt marsh, and seagrass) in ambient conditions, this function significantly plateaued and even declined with increasing oyster density when nitrate was experimentally elevated in the water column (Smyth et al., 2015). The N regeneration potential of bivalve populations are significant metrics contributing to their mitigation potential and we stress that mass deployment of bivalves is not a "one size fits all" solution to nitrogen loading. Furthermore, the effect of bivalve density on N functions may be non-linear, vary across plot to ecosystem scales and, in turn, have differing implications for the macrophytes with which they interact. We observed this variability with porewater ammonium concentrations, or the potential N bioavailability for cordgrass uptake, where values scaled logarithmically along mussel density gradients both within aggregations and across the salt marsh platform, but in opposite directions. Overall, future work is needed to disentangle conditional, density-dependent effects of bivalve species on N cycling at various scales, especially as stressors amplify under a changing climate.

Of final note, our study found that positive, density-dependent denitrification held true at the landscape scale, where mussel-enhanced nitrogen removal extended beyond their aggregations and into surrounding salt marsh areas. Thus, nitrogen removal hotspots in salt marshes may be identified based on both the size distribution of individual aggregations as well as aggregation cover across the landscape—features that can be well predicted by tidal creak features and remotely estimated (Crotty & Angelini, 2020; Pinton et al., 2023). A similar approach to resolving bivalve density dependence of N functioning should be considered in other aquatic systems, particularly where bivalves interact with foundational macrophytes that can markedly assimilate the supplemental N captured and deposited by suspension feeders or whose survival largely hinges upon water quality.

AUTHOR CONTRIBUTIONS

Sydney L. Williams, Hallie S. Fischman, Christine Angelini, and Ashley R. Smyth conceived the ideas and designed methodology; Sydney L. Williams, Hallie S. Fischman, and Ashley R. Smyth collected the data; Sydney L. Williams analysed the data; Sydney L. Williams, Christine Angelini, Ashley R. Smyth led the writing of the manuscript. All authors contributed critically to the drafts and gave final approval for publication.

ACKNOWLEDGEMENTS

We thank A. Smyth's lab members, I. Ruiz and G. Foursa, at University of Florida's Tropical Research and Education Center as well as D. Laughinghouse and his lab at the University of Florida's Fort Lauderdale Research and Education Center for providing technical expertise and support with dissolved gas and DIN analyses. We thank T. Bianchi's Organic Geochemistry Lab, E. Morrison, and J. Curtis at the University of Florida's Stable Isotope Mass Spectrometry Lab for supporting cordgrass tissue sample preparation and analysis. We also thank J. Grissett, A. Sakr, and A Bijak for field and lab support. This work was supported by NOAA Award NA20NOS4200119 to SLW, NSF CAREER Grant 1652628 to CA, and the NSF BIO OCE GCE LTER sub-award to CA. Logistical support was provided Georgia Coastal Ecosystems Long Term Ecological Research Station, the University of Georgia Marine Institute, and the Sapelo Island National Estuarine Research Reserve.

CONFLICT OF INTEREST STATEMENT

The authors declare no conflicts of interest.

PEER REVIEW

The peer review history for this article is available at https://www.webofscience.com/api/gateway/wos/peer-review/10.1111/1365-2745.14342.

DATA AVAILABILITY STATEMENT

Data and corresponding metadata from this paper as well as a comprehensive R Markdown file containing the code for this study can be found at the following Zenodo repository (Williams et al., 2024): https://doi.org/10.5281/zenodo.10561421.

ORCID

Sydney L. Williams https://orcid.org/0000-0002-9176-1838
Christine Angelini https://orcid.org/0000-0002-6669-5269

REFERENCES

Alber, M., Swenson, E. M., Adamowicz, S. C., & Mendelssohn, I. A. (2008). Salt Marsh Dieback: An overview of recent events in the US. *Estuarine, Coastal and Shelf Science*, *80*, 1–11.

Allen, D. C., & Vaughn, C. C. (2011). Density-dependent biodiversity effects on physical habitat modification by freshwater bivalves. *Ecology*, *92*, 1013–1019.

Angelini, C., Griffin, J. N., Van De Koppel, J., Lamers, L. P. M., Smolders, A. J. P., Derksen-Hooijberg, M., Van Der Heide, T., & Silliman, B. R. (2016). A keystone mutualism underpins resilience of a coastal ecosystem to drought. *Nature Communications*, *7*, 1–8.

Angelini, C., Van Heide, T. D., Griffin, J. N., Morton, J. P., Derksen-Hooijberg, M., Lamers, L. P. M., Smolders, A. J. P., & Silliman, B. R. (2015). Foundation species' overlap enhances biodiversity and multifunctionality from the patch to landscape scale in southeastern United States salt marshes. *Proceedings of the Royal Society B: Biological Sciences*, *282*, 1–9.

Annis, W. K., Hunter, E. A., & Carroll, J. M. (2022). Within-marsh and landscape features structure ribbed mussel distribution in Georgia, USA, marshes. *Estuaries and Coasts*, *45*, 2660–2674.

Ayvazian, S., Mulvaney, K., Zarnoch, C., Palta, M., Reichert-Nguyen, J., McNally, S., Pilaro, M., Jones, A., Terry, C., & Fulweiler, R. W. (2021). Beyond bioextraction: The role of oyster-mediated denitrification in nutrient management. *Environmental Science & Technology*, *55*, 14457–14465.

Aziz, S. A. A., & Nedwell, D. B. (1979). Microbial nitrogen transformations in the salt marsh environment. In R. L. Jefferies & A. J. Davy (Eds.), *Ecological processes in coastal environments* (pp. 385–398). Blackwell Scientific Publication.

Bartoli, M., Naldi, M., Nizzoli, D., Roubaix, V., & Viaroli, P. (2003). Influence of clam farming on macroalgal growth: A microcosm experiment.

Chemistry and Ecology, *19*(2–3), 147–160. https://doi.org/10.1080/02757540310001199 06

Bertness, M. D. (1984). Ribbed mussels and spartina alterniflora production in a New England salt marsh. *Ecology*, *65*, 1794–1807.

Bertness, M. D., & Callaway, R. (1994). Positive interactions in communities. *Trends in Ecology & Evolution*, *9*, 191–193.

Bertness, M. D., & Leonard, G. H. (1997). The role of positive Interations in communities: Lessons from intertidal habitats. *Ecology*, *78*, 1976–1989.

Bilkovic, D. M., Mitchell, M. M., Isdell, R. E., Schliep, M., & Smyth, A. R. (2017). Mutualism between ribbed mussels and cordgrass enhances salt marsh nitrogen removal. *Ecosphere*, *8*(4), e01795. https://doi.org/10.1002/ecs2.1795

Booth, D., & Heck, K. (2009). Effects of the American oyster *Crassostrea virginica* on growth rates of the seagrass *Halodule wrightii*. *Marine Ecology Progress Series*, *389*, 117–126.

Brandes, J. A., & Devol, A. H. (1997). Isotopic fractionation of oxygen and nitrogen in coastal marine sediments. *Geochimica et Cosmochimica Acta*, *61*, 1793–1801.

Bruno, J. F., Stachowicz, J. J., & Bertness, M. D. (2003). Inclusion of facilitation into ecological theory. *Trends in Ecology & Evolution*, *18*, 119–125.

Bulmer, R. H., Townsend, M., Drylie, T., & Lohrer, A. M. (2018). Elevated turbidity and the nutrient removal capacity of seagrass. *Frontiers in Marine Science*, *5*, 462.

Bürkner, P. (2017). brms: An R package for Bayesian multilevel models using stan. *Journal of Statistical Software*, *80*(1), 1–28. https://doi.org/10.18637/jss.v080.i01

Bürkner, P. (2018). Advanced Bayesian multilevel modeling with the R package brms. *The R Journal*, *10*(1), 395–411. https://doi.org/10.32614/RJ-2018-017

Bürkner, P. (2021). Bayesian item response modeling in R with brms and Stan. *Journal of Statistical Software*, *100*(5), 1–54. https://doi.org/10.18637/jss.v100.i05

Bürkner, P., Gabry, J., Kay, M., & Vehtari, A. (2023). posterior: Tools for working with posterior distributions. R package version 1.4.1. https://mc-stan.org/posterior/

Carlsson, M., Engström, P., Lindahl, O., Ljungqvist, L., Petersen, J., Svanberg, L., & Holmer, M. (2012). Effects of mussel farms on the benthic nitrogen cycle on the Swedish west coast. *Aquaculture Environment Interactions*, *2*, 177–191.

Carroll, J., Gobler, C., & Peterson, B. (2008). Resource-restricted growth of eelgrass in New York estuaries: Light limitation, and alleviation of nutrient stress by hard clams. *Marine Ecology Progress Series*, *369*, 51–62.

Carss, D. N., Brito, A. C., Chainho, P., Ciutat, A., de Montaudouin, X., Fernández Otero, R. M., Filgueira, M. I., Garbutt, A., Goedknegt, M. A., Lynch, S. A., Mahony, K. E., Maire, O., Malham, S. K., Orvain, F., van der Schatte Olivier, A., & Jones, L. (2020). Ecosystem services provided by a non-cultured shellfish species: The common cockle *Cerastoderma edule*. *Marine Environmental Research*, *158*, 104931.

Ciutat, A., Widdows, J., & Pope, N. D. (2007). Effect of *Cerastoderma edule* density on near-bed hydrodynamics and stability of cohesive muddy sediments. *Journal of Experimental Marine Biology and Ecology*, *346*, 114–126.

Crotty, S. M., & Angelini, C. (2020). Geomorphology and species interactions control facilitation cascades in a salt marsh ecosystem. *Current Biology*, *30*, 1562–1571.e4.

Crotty, S. M., Pinton, D., Canestrelli, A., Fischman, H. S., Ortals, C., Dahl, N. R., Williams, S., Bouma, T. J., & Angelini, C. (2023). Faunal engineering stimulates landscape-scale accretion in southeastern US salt marshes. *Nature Communications*, *14*, 881.

Derksen-Hooijberg, M., van der Heide, T., Lamers, L. P. M., Borst, A., Smolders, A. J. P., Govers, L. L., Hoogveld, J. R. H., & Angelini, C. (2018). Burrowing crabs weaken mutualism between foundation species. *Ecosystems*, *22*, 767–780.

Desmit, X., Thieu, V., Billen, G., Campuzano, F., Dulière, V., Garnier, J., Lassaletta, L., Ménesguen, A., Neves, R., Pinto, L., Silvestre, M., Sobrinho, J. L., & Lacroix, G. (2018). Reducing marine eutrophication may require a paradigmatic change. *Science of the Total Environment*, *635*, 1444–1466.

Eyre, B. D., & Ferguson, A. J. P. (2002). Comparison of carbon production and decomposition, benthic nutrient fluxes and denitrification in seagrass, phytoplankton, benthic microalgae-and macroalgae-dominated warm-temperate Australian lagoons. *Marine Ecology Progress Series*, *229*, 43–59.

Fischman, H. S., Smyth, A. R., & Angelini, C. (2023). Invasive consumers provoke ecosystem-wide disruption of salt marsh functions by dismantling a keystone mutualism. *Biological Invasions*, *26*, 169–185.

Fodrie, F. J., Rodriguez, A. B., Gittman, R. K., Grabowski, J. H., Lindquist, N. L., Peterson, C. H., Piehler, M. F., & Ridge, J. T. (2017). Oyster reefs as carbon sources and sinks. *Proceedings of the Royal Society B: Biological Sciences*, *284*(1859), 20170891.

Fry, B. (2006). *Stable isotope ecology*. Springer.

Gabry, J., Češnovar, R., & Johnson, A. (2023). _cmdstanr: R Interface to 'CmdStan'_. https://mc-stan.org/cmdstanr/, https://discourse.mc-stan.org

Gabry, J., & Mahr, T. (2022). bayesplot: Plotting for Bayesian models. R package version 1.10.0. https://mc-stan.org/bayesplot/

Gagnon, K., Rinde, E., Bengil, E. G. T., Carugati, L., Christianen, M. J. A., Danovaro, R., Gambi, C., Govers, L. L., Kipson, S., Meysick, L., Pajusalu, L., Tüney Kızılkaya, İ., van de Koppel, J., van der Heide, T., van Katwijk, M. M., & Boström, C. (2020). Facilitating foundation species: The potential for plant–bivalve interactions to improve habitat restoration success. *Journal of Applied Ecology*, *57*, 1161–1179.

Galimany, E., Wikfors, G. H., Dixon, M. S., Newell, C. R., Meseck, S. L., Henning, D., Li, Y., & Rose, J. M. (2017). Cultivation of the ribbed mussel (*Geukensia demissa*) for nutrient bioextraction in an urban estuary. *Environmental Science and Technology*, *51*, 13311–13318.

Gilbert, P. M., & Burford, M. A. (2017). Globally changing nutrient loads and harmful algal blooms: Recent advances, new paradigms, and continuing challenges. *Oceanography*, *30*, 58–69.

Gobler, C. J., Doall, M. H., Peterson, B. J., Young, C. S., DeLaney, F., Wallace, R. B., Tomasetti, S. J., Curtin, T. P., Morrell, B. K., Lamoureux, E. M., Ueoka, B., Griffith, A. W., Carroll, J. M., Nanjappa, D., Jankowiak, J. G., Goleski, J. A., Famularo, A. M. E., Kang, Y., Pikitch, E. K., … Kulp, R. E. (2022). Rebuilding a collapsed bivalve population, restoring seagrass meadows, and eradicating harmful algal blooms in a temperate lagoon using Spawner sanctuaries. *Frontiers in Marine Science*, *9*, 911731.

Goodman, P. J., & Williams, W. T. (1961). Investigations into 'Die-Back' in Spartina Townsendii Agg.: III. Physiological correlates of 'Die-Back'. *Journal of Ecology*, *49*, 391–398.

Gren, M., Lindahl, O., & Lindqvist, M. (2009). Values of mussel farming for combating eutrophication: An application to the Baltic Sea. *Ecological Engineering*, *35*, 935–945.

Hoellein, T. J., & Zarnoch, C. B. (2014). Effect of eastern oysters (*Crassostrea virginica*) on sediment carbon and nitrogen dynamics in an urban estuary. *Ecological Applications*, *24*, 271–286.

Humphries, A. T., Ayvazian, S. G., Carey, J. C., Hancock, B. T., Grabbert, S., Cobb, D., Strobel, C. J., & Fulweiler, R. W. (2016). Directly measured denitrification reveals oyster aquaculture and restored oyster reefs remove nitrogen at comparable high rates. *Frontiers in Marine Science*, *3*, 74.

Jones, H. F. E., Pilditch, C. A., Bruesewitz, D. A., & Lohrer, A. M. (2011). Sedimentary environment influences the effect of an infaunal suspension feeding bivalve on estuarine ecosystem function. *PLoS One*, *6*, e27065.

Kana, T. M., Darkangelo, C., Hunt, M. D., Oldham, J. B., Bennett, G. E., & Cornwell, J. C. (1994). Membrane inlet mass spectrometer for rapid

high-precision determination of N_2, O_2, and Ar in environmental water samples. *Analytical Chemistry*, *66*(23), 4166–4170.
Kaplan, W., Valiela, I., & Teal, J. M. (1979). Denitrification in a salt marsh ecosystem. *Limnology and Oceanography*, *24*(4), 726–734. https://doi.org/10.4319/lo.1979.24.4.0726
Kellogg, L. M., Cornwell, J. C., Owens, M. S., Luckenbach, M. W., Ross, P. G., Leggett, A. T., Dreyer, J. C., Lusk, B., Birch, A., & Smith, E. (2014). *Scaling ecosystem services to reef development: Effects of oyster density on nitrogen removal and reef community structure*. Virginia Institute of Marine Science.
Kemp, W. M., Sampou, P., Caffrey, J., Mayer, M., Henriksen, K., & Boynton, W. R. (1990). Ammonium recycling versus denitrification in Chesapeake Bay sediments. *Limnology and Oceanography*, *35*(7), 1545–1563. https://doi.org/10.4319/lo.1990.35.7.1545
Koop-Jakobsen, K., & Giblin, A. E. (2010). The effect of increased nitrate loading on nitrate reduction via denitrification and DNRA in salt marsh sediments. *Limnology and Oceanography*, *55*(2), 789–802. https://doi.org/10.4319/lo.2010.55.2.0789
Kotta, J., Futter, M., Kaasik, A., Liversage, K., Rätsep, M., Barboza, F. R., Bergström, L., Bergström, P., Bobsien, I., & Díaz, E. (2020). Cleaning up seas using blue growth initiatives: Mussel farming for eutrophication control in the Baltic Sea. *Science of the Total Environment*, *709*, 136144.
Kuenzler, E. J. (1961). Structure and energy flow of a mussel population in a Georgia salt marsh. *Limnology and Oceanography*, *6*, 191–204.
Laverock, B., Gilbert, J. A., Tait, K., Osborn, A. M., & Widdicombe, S. (2011). Bioturbation: Impact on the marine nitrogen cycle. *Biochemical Society Transactions*, *39*, 315–320.
Lin, J. (1989). Influence of location in a salt marsh on survivorship of ribbed mussels. *Marine Ecology Progress Series. Oldendorf*, *56*, 105–110.
Lindahl, O., Hart, R., Hernroth, B., Kollberg, S., Loo, L.-O., Olrog, L., Rehnstam-Holm, A.-S., Svensson, J., Svensson, S., & Syversen, U. (2005). Improving marine water quality by mussel farming: A profitable solution for Swedish society. *AMBIO: A Journal of the Human Environment*, *34*, 131–138.
Lunstrum, A., McGlathery, K., & Smyth, A. (2018). Oyster (*Crassostrea virginica*) aquaculture shifts sediment nitrogen processes toward mineralization over denitrification. *Estuaries and Coasts*, *41*, 1130–1146.
Marinelli, R. L., & Williams, T. J. (2003). Evidence for density-dependent effects of infauna on sediment biogeochemistry and benthic–pelagic coupling in nearshore systems. *Estuarine, Coastal and Shelf Science*, *57*, 179–192.
Matheson, F. E., Nguyen, M. L., Cooper, A. B., Burt, T. P., & Bull, D. C. (2002). Fate of 15N-nitrate in unplanted, planted and harvested riparian wetland soil microcosms. *Ecological Engineering*, *19*, 249–264.
Moore, A. F. P., & Hughes, A. R. (2023). Asymmetrical facilitation ameliorates environmental conditions through positive feedback in partner traits. *Ecosphere*, *14*, e4560.
Murphy, A., Anderson, I., & Luckenbach, M. (2015). Enhanced nutrient regeneration at commercial hard clam (*Mercenaria mercenaria*) beds and the role of macroalgae. *Marine Ecology Progress Series*, *530*, 135–151.
Murphy, A. E., Anderson, I. C., Smyth, A. R., Song, B., & Luckenbach, M. W. (2016). Microbial nitrogen processing in hard clam (*Mercenaria mercenaria*) aquaculture sediments: The relative importance of denitrification and dissimilatory nitrate reduction to ammonium (DNRA). *Limnology and Oceanography*, *61*, 1589–1604.
Murphy, A. E., Emery, K. A., Anderson, I. C., Pace, M. L., Brush, M. J., & Rheuban, J. E. (2016). Quantifying the effects of commercial clam aquaculture on C and N cycling: An integrated ecosystem approach. *Estuaries and Coasts*, *39*, 1746–1761.
Newell, R. (2004). Ecosystem influences of natural and cultivated populations of suspension-feeding bivalve molluscs: A review. *Journal of Shellfish Research*, *23*, 51–61.
Nizzoli, D., Welsh, D., Fano, E., & Viaroli, P. (2006). Impact of clam and mussel farming on benthic metabolism and nitrogen cycling, with emphasis on nitrate reduction pathways. *Marine Ecology Progress Series*, *315*, 151–165.
Ogburn, M. B., & Alber, M. (2006). An investigation of salt marsh dieback in Georgia using field transplants. *Estuaries and Coasts*, *29*, 54–62.
Peterson, B. J., & Heck, K. L. (2001). Positive interactions between suspension-feeding bivalves and seagrass—A facultative mutualism. *Marine Ecology Progress Series*, *213*, 143–155.
Pinton, D., Canestrelli, A., Williams, S., Angelini, C., & Wilkinson, B. (2023). Estimating mussel mound distribution and geometric properties in coastal salt marshes by using UAV-Lidar point clouds. *Science of the Total Environment*, *883*, 163707.
R Core Team. (2023). *R: A language and environment for statistical computing*. R Foundation for Statistical Computing. https://www.R-project.org/
Reisinger, A. J., Tank, J. L., Hoellein, T. J., & Hall, R. O. (2016). Sediment, water column, and open-channel denitrification in rivers measured using membrane-inlet mass spectrometry. *Journal of Geophysical Research: Biogeosciences*, *121*, 1258–1274.
Reusch, T. B., Chapman, A. R., & Gröger, J. P. (1994). Blue mussels Mytilus edulis do not interfere with eelgrass *Zostera marina* but fertilize shoot growth through biodeposition. *Marine Ecology Progress Series*, *108*, 265–282.
Rossi, R. E., Schutte, C. A., Logarbo, J., Bourgeois, C., & Roberts, B. J. (2022). Gulf ribbed mussels increase plant growth, primary production, and soil nitrogen cycling potential in salt marshes. *Marine Ecology Progress Series*, *689*, 33–46.
Sandwell, D. R., Pilditch, C. A., & Lohrer, A. M. (2009). Density dependent effects of an infaunal suspension-feeding bivalve (*Austrovenus stutchburyi*) on sandflat nutrient fluxes and microphytobenthic productivity. *Journal of Experimental Marine Biology and Ecology*, *373*, 16–25.
Schröder, T., Stank, J., Schernewski, G., & Krost, P. (2014). The impact of a mussel farm on water transparency in the Kiel Fjord. *Ocean and Coastal Management*, *101*, 42–52.
Sharp, S. J., & Angelini, C. (2016). Whether disturbances alter salt marsh soil structure dramatically affects Spartina alterniflora recolonization rate. *Ecosphere*, *7*, e01540.
Smyth, A. R., Geraldi, N. R., & Piehler, M. F. (2013). Oyster-mediated benthic-pelagic coupling modifies nitrogen pools and processes. *Marine Ecology Progress Series*, *493*, 23–30.
Smyth, A. R., Murphy, A. E., Anderson, I. C., & Song, B. (2018). Differential effects of bivalves on sediment nitrogen cycling in a shallow Coastal Bay. *Estuaries and Coasts*, *41*, 1147–1163.
Smyth, A. R., Piehler, M. F., & Grabowski, J. H. (2015). Habitat context influences nitrogen removal by restored oyster reefs. *Journal of Applied Ecology*, *52*, 716–725.
Stan Development Team. (2023). Stan modeling language users guide and reference manual, version 2.32. https://mc-stan.org
Stiven, A. E., & Gardner, S. A. (1992). Population processes in the ribbed mussel *Geukensia demissa* (Dillwyn) in a North Carolina salt marsh tidal gradient: Spatial pattern, predation, growth and mortality. *Journal of Experimental Marine Biology and Ecology*, *160*, 81–102.
Temmink, R. J. M., Angelini, C., Verkuijl, M., & Van Der Heide, T. (2023). Restoration ecology meets design-engineering: Mimicking emergent traits to restore feedback-driven ecosystems. *Science of the Total Environment*, *902*, 166460.
Testa, J., Brady, D., Cornwell, J., Owens, M., Sanford, L., Newell, C., Suttles, S., & Newell, R. (2015). Modeling the impact of floating oyster (*Crassostrea virginica*) aquaculture on sediment-water nutrient and oxygen fluxes. *Aquaculture Environment Interactions*, *7*, 205–222.
Thornton, S. F., & McManus, J. (1994). Application of organic carbon and nitrogen stable isotope and C/N ratios as source indicators of organic matter provenance in estuarine systems: Evidence from the Tay Estuary, Scotland. *Estuarine, Coastal and Shelf Science*, *38*, 219–233.

Wagner, E., Dumbauld, B. R., Hacker, S. D., Trimble, A. C., Wisehart, L. M., & Ruesink, J. L. (2012). Density-dependent effects of an introduced oyster, *Crassostrea gigas*, on a native intertidal seagrass, *Zostera marina*. *Marine Ecology Progress Series*, *468*, 149–160.

Williams, S. L., Fischman, H. S., Angelini, C., & Smyth, A. R. (2024). Density-dependent influence of ribbed mussels on salt marsh nitrogen pools and processes (v1.0.2). *Zenodo*. https://doi.org/10.5281/zenodo.10561484

Williams, S. L., Rogers, J. L., Fischman, H. S., Morrison, E. S., & Angelini, C. (2023). The role of a faunal engineer, *Geukensia demissa*, in modifying carbon and nitrogen regulation Services in Salt Marshes. *Journal of Geophysical Research: Biogeosciences*, *128*, e2023JG007535.

Wurtsbaugh, W. A., Paerl, H. W., & Dodds, W. K. (2019). Nutrients, eutrophication and harmful algal blooms along the freshwater to marine continuum. *WIREs Water*, *6*, e1373.

Zhou, J., Wu, Y., Zhang, J., Kang, Q., & Liu, Z. (2006). Carbon and nitrogen composition and stable isotope as potential indicators of source and fate of organic matter in the salt marsh of the Changjiang Estuary, China. *Chemosphere*, *65*, 310–317.

Zhou, Y., Yang, H., Zhang, T., Qin, P., Xu, X., & Zhang, F. (2006). Density-dependent effects on seston dynamics and rates of filtering and biodeposition of the suspension-cultured scallop *Chlamys farreri* in a eutrophic bay (northern China): An experimental study in semi-in situ flow-through systems. *Journal of Marine Systems*, *59*, 143–158.

Zhu, J., Zarnoch, C., Gosnell, J., Alldred, M., & Hoellein, T. (2019). Ribbed mussels *Geukensia demissa* enhance nitrogen-removal services but not plant growth in restored eutrophic salt marshes. *Marine Ecology Progress Series*, *631*, 67–80.

SUPPORTING INFORMATION

Additional supporting information can be found online in the Supporting Information section at the end of this article.

Figure S1. Map of Old Teakettle Creek study site, located near Sapelo Island, Georgia (USA).

Figure S2. Bar charts depict mean crab burrow density (a) and cordgrass stem density (b) surveyed in mussel aggregations (light brown) and cordgrass only plots (light green).

Figure S3. Graphs show calculated denitrification efficiencies for microcosm incubation samples collected from mussel aggregations (light brown; a) and cordgrass only plots (light green; b).

Table S1. Summary of Bayesian model frameworks, including model formulas, response distributions, link functions, estimated coefficients, and uncertainty intervals.

How to cite this article: Williams, S. L., Fischman, H. S., Angelini, C., & Smyth, A. R. (2024). Density-dependent influence of ribbed mussels on salt marsh nitrogen pools and processes. *Journal of Ecology*, *112*, 1599–1612. https://doi.org/10.1111/1365-2745.14342